

Mapping of the potential fluctuations by multiple-tip probes on the CASTOR tokamak

V. Svoboda, FJFI ČVUT, Prague
J. Stöckel, F. Žáček, Institute of Plasma Physics, Prague

- Introduction
- Motivation: Trajectories of Test Particles in the Potential Landscape Due to $\vec{E}_{rad} \times \vec{B}_{tor}$ - drift;
- Characterization of Potential Fluctuations by Poloidal and Radial Probe Arrays;
- Space-Time Correlation Analysis;
- Summary

References:

1. Bellan P.M.: "Transport inferred from consideration of particle orbits in drift turbulence", Plasma Phys. and Contr. Fus., 35, 1993, No.2, 169-178
2. Isichenko M.B., Horton W.: "Scaling laws of stochastic ExB plasma transport", Comments on Plasma Phys. and Contr. Fusion, 14, 1991, No.5, p.249-262
3. Tao Y.Q., Conn R.W., Schmitz L., Tynan G.: "Ion flow in a sheared electric field", Phys. Fluids, B5 (2), 1993, p. 344-349.
4. Zweben S.J., Gould R.W.: Structure of Edge-Plasma Turbulence in the CALTECH tokamak, Nucl. Fusion, 25, (1985), No.2, p. 171
5. Zweben S.J.: Search for Coherent Structure Within Tokamak Plasma Turbulence, Phys. Fluids, 28(3), 1985, p.974
6. Endler M., Giannone L., Niedermayer H., Rudyj, Theimer G. and the ASDEX team, Experimental and theoretical investigation of density and potential fluctuations in the scrape-off layer of ASDEX; In Proc. of 20th EPS Conference on Controlled Fusion and Plasma, Lisbon 1993, Part II. p. 583

z:il.cz

Cíl experimentu

- Fluktuace potenciálu plazmatu
 - Charakterizovat jednu komponentu elektrostatické turbulence okrajového plazmatu - fluktuace potenciálu plazmatu;
 - Stanovit zejména:
 - * charakteristickou dobu života poruch potenciálu (prozatím v laboratorní souřadné soustavě)
 - * charakteristický rozměr poruch potenciálu jak v poloidálním tak i radiálním směru;
 - * velikost a smysl rotace poruch potenciálu v poloidálním směru
- Experimentální uspořádání
 - Tokamak CASTOR
 - Mnohahrotové Langmuirovy sondy umožňující mapovat plovoucí potenciál plazmatu během jediného výstřelu jak v radiálním tak i poloidálním směru;
 - Rychlá a mnohakanálová digitalizace signálů z jednotlivých hrotů (8 kanálů, 4096 vzorků na kanál, 1μs/vzorek)
- Zpracování experimentálních dat
 - korelační analýza signálů z jednotlivých hrotů - výpočet korelačních funkcí

Motivace

• Udržení plazmatu a turbulence

- Klíčový parametr charakterizující kvalitu udržení plazmatu v magnetických nádobách je doba udržení energie (částic)

$$\tau_E = Q/\Gamma_E \quad \tau_p = N/\Gamma_p$$

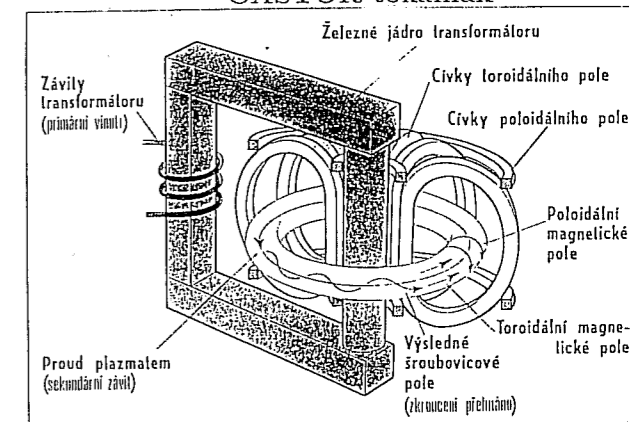
kde Q resp N je celková energie resp celkový počet částic v nádobě a Γ_E resp Γ_p jsou celkové toky energie resp částic na stěnu nádoby;

- Celkové toky jsou úměrné zejména velikosti koeficientů tepelné vodivosti χ resp difuze D;
- Jak se ukázalo, jsou transportní koeficienty 100 až 1000krát větší než teoretické hodnoty;
- To je hlavní překážkou uskutečnění řízeného slučování v magnetických nádobách typu tokamaků;
- Má se obecně za to, že anomálně vysoký transport je způsoben turbulentí plazmatu;

• Okrajová slupka plazmatu

- Principiální význam pro globální udržení mají okrajové vrstvy plazmatu, neboť toky energie a částic na stěny komory musí protékat okrajovou slupkou;
- Dominantní proces ovlivňující transport okrajovou slupkou je elektrostatická turbulence plazmatu (fluktuace hustoty, potenciálu a teploty);
- Na kraji sloupce plazmatu možno vytvořit transportní bariéru - prokázáno experimentálně při tzv. H-mode operation (poloidální rotace plazmatu → potlačení turbulence → omezení radiálního transportu → zlepšení globálního udržení plazmatu);
- Podstata okrajové turbulence není doposud zcela vyjasněna; neexistuje teoretický popis plně postihující experiment;
- Jednou z příčin je nedostatek údajů charakterizujících turbulence

CASTOR tokamak



Major radius: $R = 40$ cm Minor radius: $a = 8.5$ cm
Toroidal magnetic field: $B = 1$ T Plasma current: $I_p = 10 - 20$ kA
Density: $\bar{n} = 2 - 20 \cdot 10^{18} \text{ m}^{-3}$
Temperature: $T_e = 200 - 400$ eV $T_i = 50 - 100$ eV

Current Drive on the CASTOR tokamak

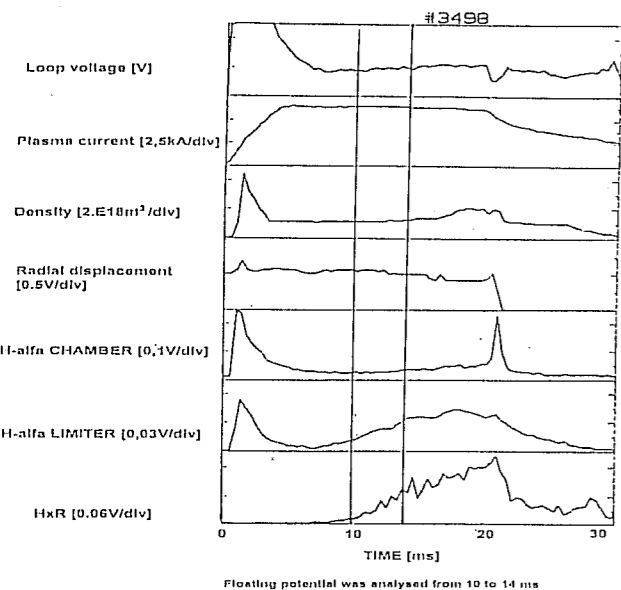
- Inductive current drive (OH)- using the tokamak transformer

$$E = -\frac{1}{2\pi R} \frac{d\Phi}{dt} \text{ --- toroidal electric field}$$

$$E = U_{loop} / 2\pi R \text{ --- loop voltage}$$

- Non-inductive current drive - using a slowed-down electromagnetic wave launched into the plasma.
antenna: multijunction waveguide grill
frequency: $f = 1.25$ GHz; ($\lambda = 24$ cm) --- Lower Hybrid Range
phase velocity: (calculated): $v_{ph} \approx c/3$
LH power: $P_{LH} < 40$ kW
LHCD efficiency: $\eta = 0.25 \text{ A/W}$ at $\bar{n}_e = 6 \cdot 10^{18} \text{ m}^{-3}$

EVOLUTION OF THE OH SHOT



Floating potential was analyzed from 10 to 14 ms

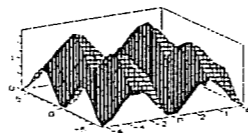
Ion Trajectory in the 2D-potential landscape

Having orthogonal system linked with rotated plasma \Rightarrow there is not necessary to consider quasistationary radial electric field.

Model of the potential landscape:

$$\phi_s(x, y) = U_0[\sin^2(kx) + \sin^2(ky)] \quad (1)$$

$k = 2\pi/\lambda$ describes the distance between the maxima or the minima of the potential.



The equation of motion for a test particle (e.g. an impurity ion)

$$m\vec{a} = q(\vec{E} + \vec{v} \times \vec{B}) \quad (2)$$

where

$$\vec{E} = (E_x, E_y, 0) \text{ and } \vec{B} = (0, 0, B) \quad (3)$$

for the each component of the vector

$$\ddot{x} = \frac{q}{m}(E_x + \dot{y}B) \quad \ddot{y} = \frac{q}{m}(E_y - \dot{x}B)$$

where

$$E_x = -\partial\phi_s/\partial x = -U_0k \cdot \sin(2kx) \quad E_y = -\partial\phi_s/\partial y = -U_0k \cdot \sin(2ky)$$

\Rightarrow

$$\ddot{x} = +\omega_{ci}[\dot{y} - v_d \cdot \sin(2kx)] \quad \ddot{y} = -\omega_{ci}[\dot{x} + v_d \cdot \sin(2ky)] \quad (4)$$

where

$\omega_{ci} = qB/m_i$ — ion cyclotron frequency

$v_d = U_0k/B$ — charakteristic velocity of the $\vec{E} \times \vec{B}$ drift

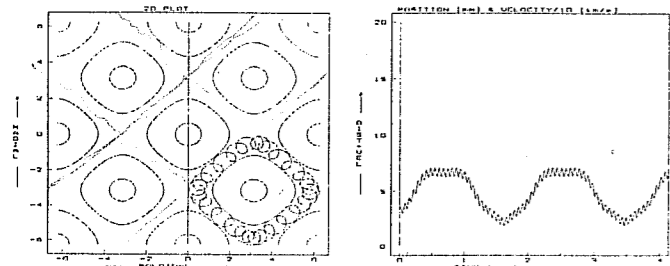
Ion trajectory in the 2D potential landscape

The equations (3) is numerically computed using practical units: time... μ s, distance x ...mm, speed \dot{x} ...mm/ μ s, potential ... Volts, magnetic field... Tesla. For hydrogen $\omega_{ci} = qB/m_i = 95.8 \cdot B$ [rad/ μ s], drift speed $v_d = U_0k/B$ is typically 5 - 50 mm/ μ s.

Final form of the equation of motion for $B = 1$ T (CASTOR) is

$$\ddot{x} = +95.8[\dot{y} - v_d \cdot \sin(2kx)] \quad \ddot{y} = -95.8[\dot{x} + v_d \cdot \sin(2ky)]$$

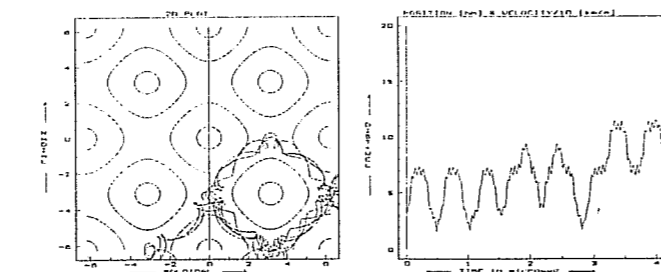
The Fig. 1. shows test partical trajectory (proton), which starts from the $(x_0, y_0) = (3.14, 0)$ (the minimum between two maxima) with initial velocity components $\dot{x} = 40$ mm/ μ s and $\dot{y} = 0$. This velocity corresponds to the proton thermal velocity at $T_i = 16$ eV. The maximum potential is chosen as $U_0 = 20$ V, the distance between maxima is $\lambda = \pi/k = 6.28$ mm, ($k = 0.5$ mm $^{-1}$).



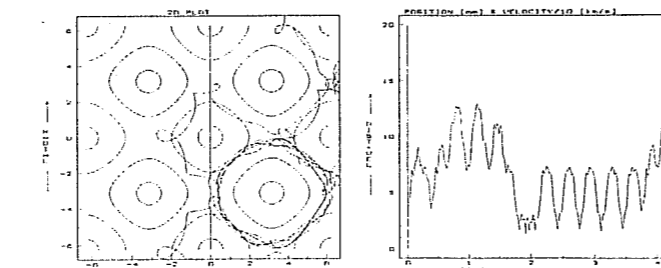
The vortex trajectory is the superposition of the cyclotron motion (with Larmor radius $r \approx 0.5$ mm) and circumnavigation around a selected potential maximum (minimum). Trajectory is frozen to a local potential hill (valley). Time of the circumnavigation is about 1.8 μ s.

Stochastic trajectory

If the drift velocity is high enough, the test particle begins to move randomly in the potential landscape.
 $U_0 = 80$ V, $k = 0.5$ mm $^{-1}$



$U_0 = 120$ V, $k = 0.5$ mm $^{-1}$



Experimental Set-Up. (poloidal probe)

Electrostatic fluctuations are monitored by a "rake" probe with 18 tips. The probe is located at the top of the torus, 40° toroidally away from the limiter section. The tips are oriented in the poloidal direction

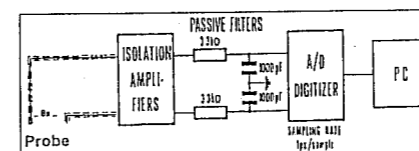
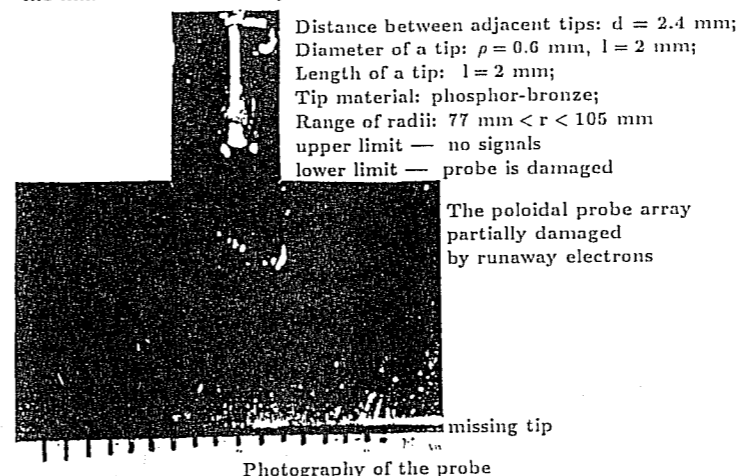
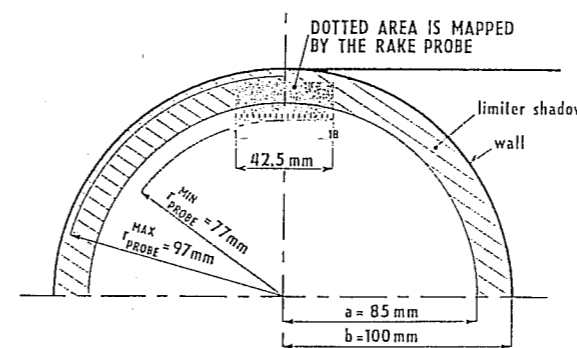


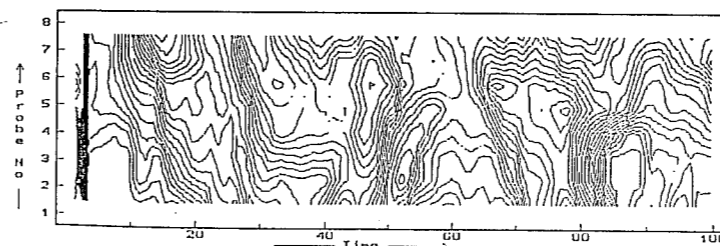
Figure 1: Electrical arrangement of the experiment

Poloidal probe array

Tip length/diameter 2/0.5 mm, distance of the adjacent tips 2.5 mm



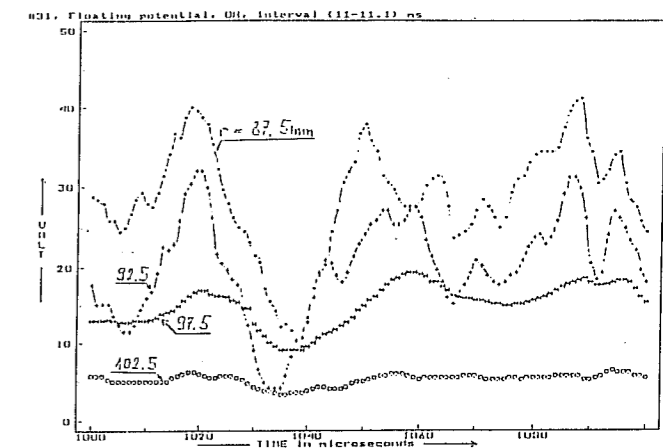
2D map of raw signals



Sampling rate 1 μ s/sample, 4096 samples
red lines - propagation in the ion diamagnetic drift direction
green lines - propagation in the electron diamagnetic drift direction

Floating probe's signals (the multitip probe in the radial direction)

Evolution of the floating potential from four tips at different positions with respect to the plasma center.

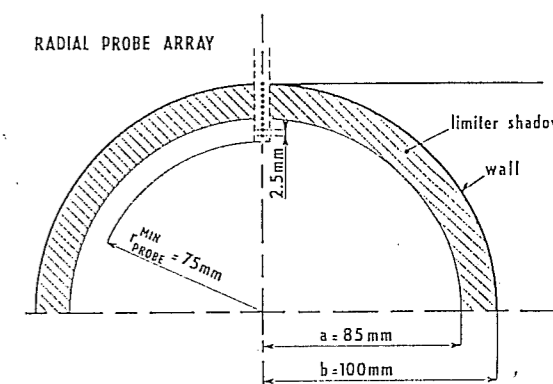


Observed signal fluctuations from individual tips are the result of three processes:

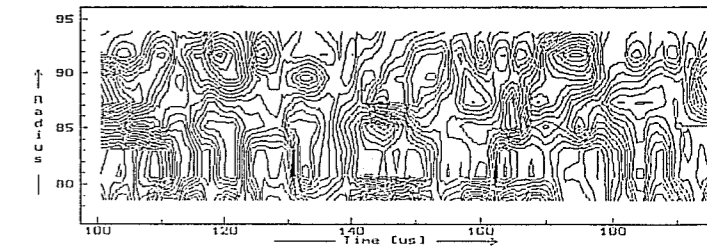
- Poloidal rotation of the "potential landscape" as the whole in laboratory frame (caused by the $\langle \vec{E}_{rad} \rangle \times \vec{B}_{tor}$ drift);
- Random motion of the single potential "hill/valley" in the frame linked with the rotating plasma;
- Finite life-time of the individual "hill/valley".

Radial probe array

Tip length/diameter 2/0.5 mm, distance of the adjacent tips 2.5 mm



2D map of raw signals



Sampling rate 1 μ s/sample, 4096 samples

Radial profile of floating potential (by the poloidal array)

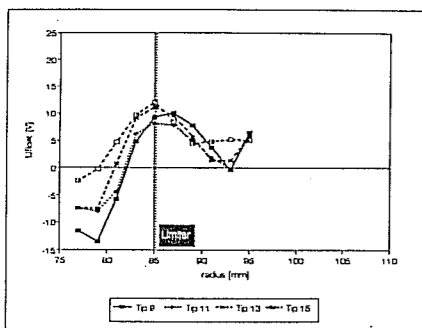


Figure 1: Radial profile of floating potential

- The floating potential (time averaged over 4 ms) is monitored in a shot to shot bases (10 shots) at different poloidal locations (the distance between the active tips is 5 mm);
- The poloidal array is not identical with a magnetic surface;
- Note the poloidal nonuniformities at $r \approx 82$ mm and $r \approx 94$ mm indicating an existence of local and quasistationary electric fields in the poloidal direction.

Radial profile of floating potential (by the radial array)

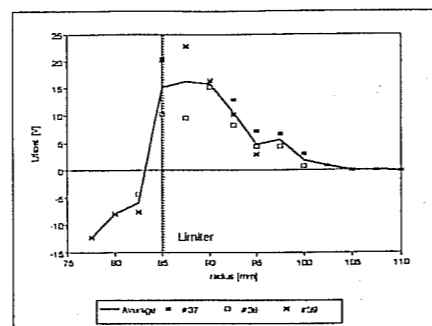


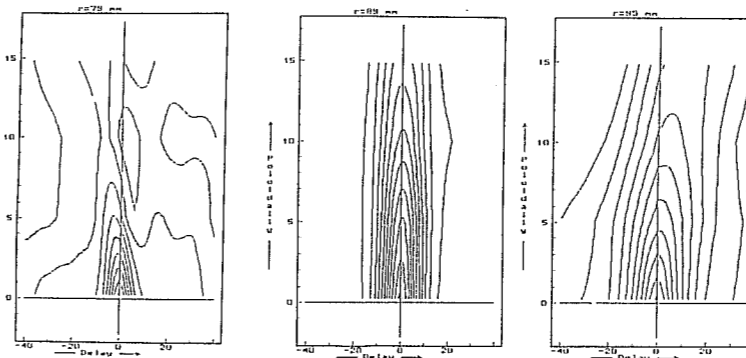
Figure 1: Radial profile of floating potential

- The floating potential (time averaged over 4 ms) is monitored in three ohmic shots.
- The electron temperature profile is nearly flat at $r = 75-95$ mm = the radial electric field $E_r = -\partial V_n / \partial r$ in this region.

In general:
 $E_r > 0$ in SOL
 $E_r < 0$ within the plasma
 Note the local changes in E_r at $r \approx 97$ mm.

Space-time correlation (by the poloidal array)

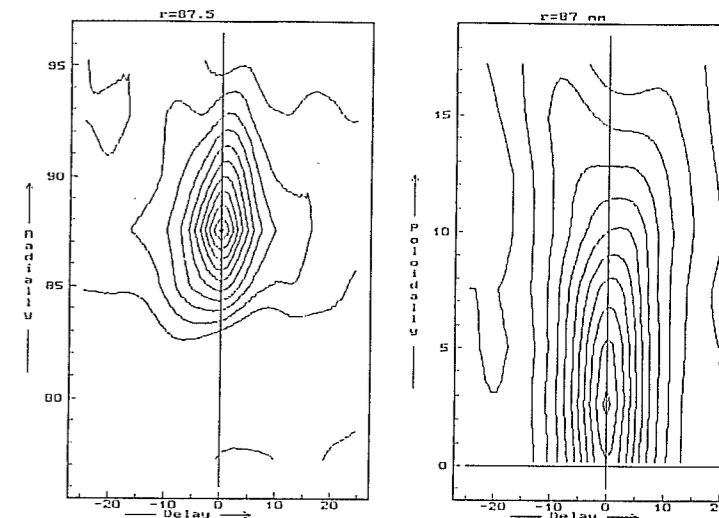
- Space-time correlation is calculated for four tips spaced poloidally;
- Distance between the adjacent probes is 5 mm;
- Distance from the reference probe d at which the crosscorrelation function drops to 0.6 is determined (for the zero time delay). The correlation length is defined as $\lambda = 2d$;
- Similarly, the correlation time is derived



- potential fluctuations propagate in the ion diamag. drift direction in SOL. Their poloidal correlation length in the range of 1-2 cm.
- Noticeably shorter λ_p is deduced for fluctuations moving in the electron diamag. drift direction $r < a$.

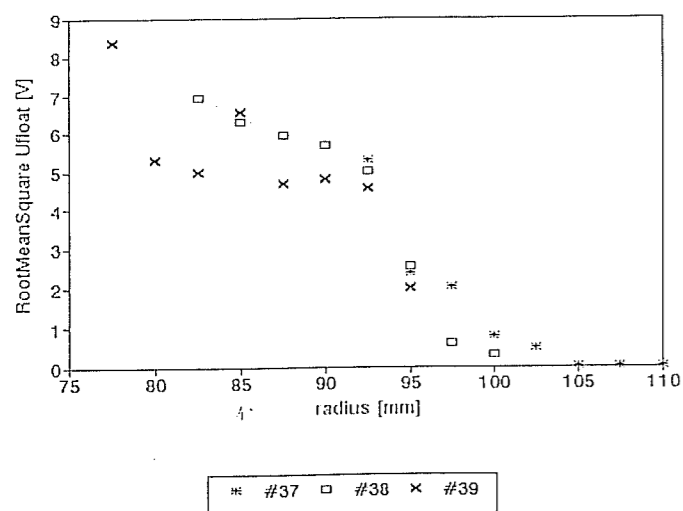
Comparison of space-time correlation in the poloidal and radial directions

- Space-time correlation is calculated for eight tips spaced poloidally/radially by 2.5 mm;
- poloidal array is located at the same radius as the reference tip of the radial array, $r \approx 87$ mm



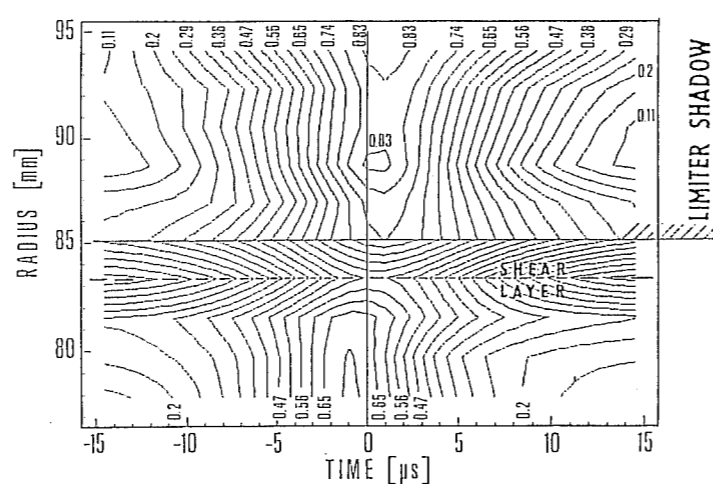
- Difference in the space correlation between the poloidal and radial directions is apparent

RMS value of the potential fluctuations (by the radial array)



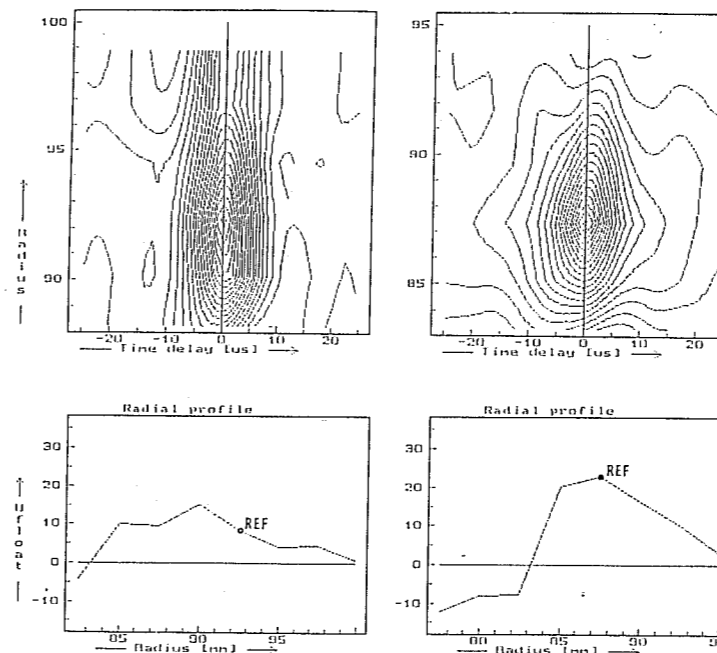
- Relative level of potential fluctuations is $\bar{\phi} / kT_e \approx 0.5$ at the limiter radius

Poloidal correlation of potential fluctuations (radial scan)



- Crosscorrelation function of potential fluctuations is calculated for tips 1 and 3 (poloidal array, the tip 1. is taken as the reference one);
- 2D map of the crosscorrelation function (radius-delay) is constructed on the shot to shot basis (10 shots);
- Poloidal propagation of fluctuations due to $\vec{E}_r \times \vec{B}_t$ drift is evident: $r > 83$ mm \Rightarrow ion diamag. drift direction; $r < 83$ mm \Rightarrow electron diamag. drift direction;
- Poloidal velocity is in the range of 1-2 km/s, which corresponds to measured radial electric fields $E_r \leq \pm 2$ kV/m;
- Velocity shear layer is located near LCPS.

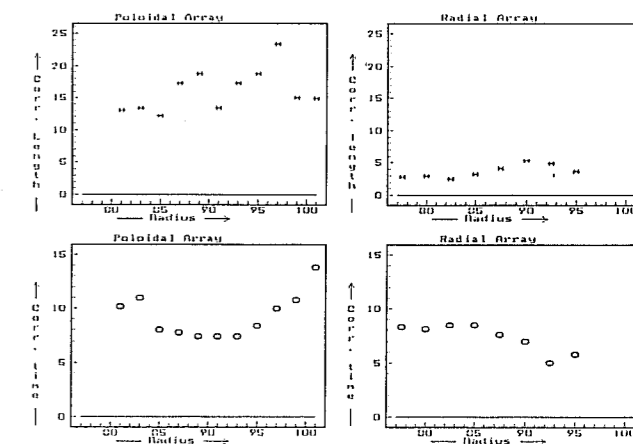
Radial propagation of fluctuations



- Space time correlation is calculated for five tips spaced radially;
- In the most cases, the propagation of fluctuations in the radial direction is not observed (the left figure);
- Under some (but still not specified) conditions, the propagation of fluctuations in the outward direction can be identified (the right figure).

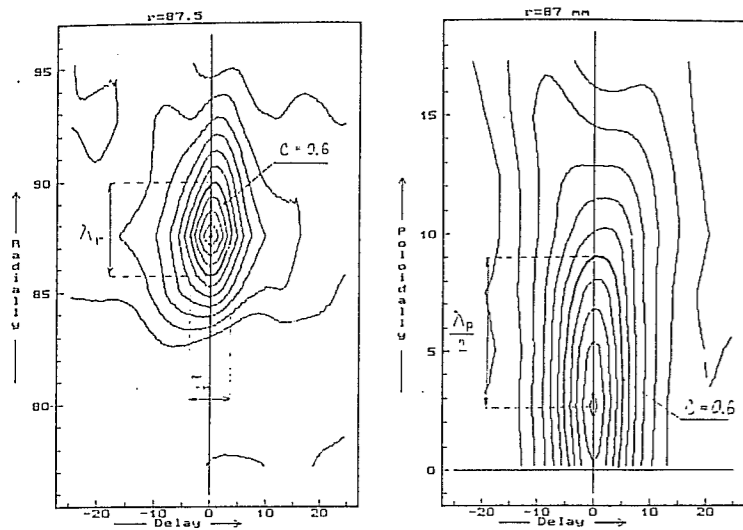
Summary of correlation analysis on the CASTOR tokamak

- Space-time correlation is calculated for eight tips spaced poloidally/radially by 2.5 mm;
- Data from the poloidal array are obtained on a shot to shot basis;
- Data from the radial array are obtained in a single shot.

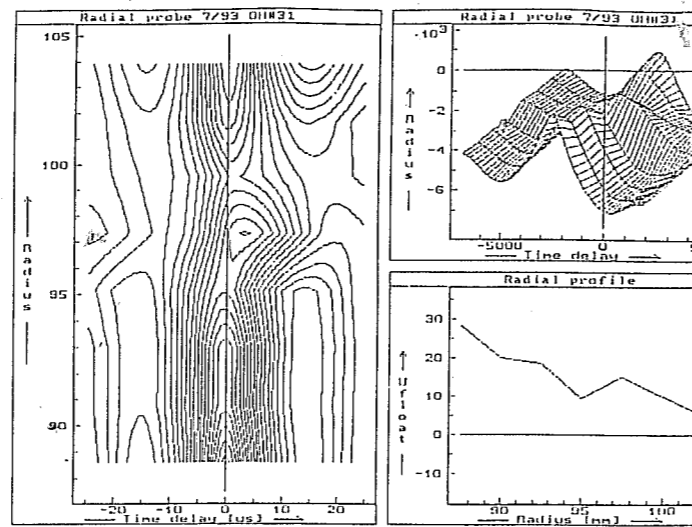


in the poloidal and radial directions

- Space-time correlation is calculated for eight tips spaced poloidally/radially by 2.5 mm;
- poloidal array is located at the same radius as the reference tip of the radial array, $r \approx 87$ mm



- Difference in the space correlation between the poloidal and radial directions is apparent



- The most inner tip $r = 87.5$ mm is taken as the reference one;
- The radial propagation (outward) of potential fluctuations appears at $r \approx 97.5$ mm;
- It demonstrates an influence of the local (quasistationary) electric fields on the motion of the potential fluctuations (see the right bottom insert).

SUMMARY

Edge plasma is investigated by Langmuir probes on the CASTOR tokamak. The three approaches have been tested to understand better the edge electrostatic turbulence in tokamaks:

- Dimensional analysis
 - Dimensionality of density fluctuations was evaluated in regimes differing in the level of fluctuations;
 - The lowest dimensionality is observed in the standard ohmic regime;
 - The link between the dimensionality and autocorrelation time is observed.
- Space-time correlation
 - Potential fluctuations were analyzed by multiple tip Langmuir probes in the poloidal and radial directions;
 - Correlation length/time was determined in both cases;
 - Radial correlation length is noticeably shorter than the poloidal one.
- Electron temperature by oscillatory technique
 - The strictly local value of T_e by the oscillatory technique well corresponds to the triple probe results;
 - Temporal resolution is limited (> 1.3 ms);
 - Mapping of the electron temperature and determination of the T_e -fluctuations on the CASTOR is envisaged.

Acknowledgement:

Work was performed under the Grant Agency of Czech Republic No. 202/93/0711 and supported by IAEA Contract 6702/r1/rb.